The contact-less method of chip-to-chip high speed data transmission monitoring

M. ZMUDA*, S. SZCZEPAŃSKI, S. KOZIEŁ, and S. GRACZYK

Faculty of Electronics, Telecommunications and Informatics, Gdańsk University of Technology,
11/12 Narutowicza St., 80-233 Gdańsk, Poland

Abstract. This paper presents a technique of decoupling differential signals transmitted in a pair of microstrip lines on a printed circuit board (PCB), using dedicated coupler for high speed data transmission monitoring in chip-to-chip interconnections. The coupler used for signal probing is overlayed on the pair of microstrip lines under test, and provides a signal to the next blocks of the measurement system without disturbing transmission in the lines. Starting from the basic configuration obtained in the previous work, we describe a procedure of re-designing the coupler for enhanced directivity so that it is suitable for high-speed data transmission monitoring. The new coupler structure has improved topology based on stepped-impedance resonators with geometry parameters adjusted using numerical optimization techniques. The correctness of the design has been confirmed by the time-domain measurements performed for real chip-to-chip communication signals, using a dedicated measurement system based on Xilinx Virtex-6 FPGA Development Kit. The presented technology can be used for reducing the cost of the product diagnostics by eliminating dedicated measurement connectors, run-time system debugging or reverse engineering.

Key words: high speed data transmission monitoring, microstrip coupler, connector-less transmission monitoring, time-domain measurements.

1. Introduction

The debugging process of high speed data links is becoming more and more difficult. Modern devices require extremely fast chip-to-chip interconnections. Often, the major bottleneck which limits the system performance is related to connections on PCBs (Printed Circuit Board) [1]. The limited bandwidth, mismatched terminations on the receiver (Rx) or transmitter (Tx) side, cross-talks, interferences from other parts of a system, differences in a transmission line length for multi-conductor transmission which causes the disturbance of phase relations, can significantly reduce the maximum transmission rate which is available with a given bit error rate (BER) [2]. This situation drives researchers to looking for new solutions [3–5].

An important aspect of improving the high-speed interconnection performance is to ensure that the prototype and production model signal an integrity debug process which allows for finding the real root cause. Various reasons (e.g., malfunction of Tx and/or Rx, the rapid change of the line impedance, Tx/Rx mismatch, interference from other devices) may result in various problems in a transmission quality, including excessive BER or interfering other devices on PCB. Attempts to solve problems that are based on general symptoms of the defect, can, in many cases, result in incorrect conclusions. Some problems can only be detected by using special signal sequences or when a particular situation occurs in the adjacent subsystem e.g., in poorly designed links,

considerably large error rates may appear for specific symbol sequences due to inter-symbol-interferences (ISI) [6]. Therefore, real-time debugging techniques become indispensable in many cases [7, 8].

The problems associated with launching the new systems, such as those mentioned in the previous passage, result in a situation where more and more designers develop their projects to comply with generally accepted standards and investigate the compliance of the design with these particular standards. Another incentive for this approach is wide availability of tools to verify compatibility with the common industrial standards, which can significantly speed up the design and launching process. Regardless of the specific approach adopted by the designer, the most crucial element of the measurement environment employed to debug the system is a connector, which, beside of the limited bandwidth, can significantly affect the measured transmission. A possible solution to this problem are socket-less signal probing techniques [7, 9] that have been rapidly developed over the last several years, and use dedicated heads which are applied to the dedicated pads on board for signal probing. While this approach eliminates the need of installing dedicated connectors for signal probing, it requires adding special pads to the layout.

In this work, we present a technique of decoupling the differential signal transmitted in a pair of microstrip lines on a PCB using a dedicated coupler [10, 11]. This approach allows us to monitor serial high speed transmission without the

*e-mail: marek.zmuda@intel.com

necessity of using any measurement connector on the board or dedicated pads for signal probing. The main task of the coupler is to deliver the probed signal to the subsequent components of the measurement system. It is important characteristic include ensuring sufficient level of the measured signal decoupling without degrading transmission in the main line. Additionally, its mechanical construction should make it possible to conveniently attach it to the circuit under testing. The decoupled signal can be then easily processed by external measurement instrumentation.

In order to make the coupler suitable for high-speed data transmission monitoring, the initial topology presented in [8] is redesigned, and its geometry parameters are adjusted using numerical optimization techniques. This optimization process, which is described in detail in the paper, results in improving the signal probing capabilities as compared to the initial structure presented in [11]. The re-designed coupler structure has been verified by the time-domain measurements obtained for real signals for chip-to-chip communications obtained with dedicated measurement system developed using Xilinx Virtex-6 FPGA Development Kit [12]. In particular, the obtained results confirm the correctness of the coupler design and the validity of the optimization process. The technology presented in this work can be used for reducing the cost of the product diagnostic by eliminating dedicated measurement connectors, run-time system debugging or reverse engineering.

The paper is organized as follows. The concept of the differential signal coupler for measurement results is presented in Sec. 2. Section 3 describes the coupler's design and its geometry optimization targeted at improving the directivity. Time domain measurement results obtained for the real chip-to-chip PCB interconnection with both couplers original and optimized) are presented in Sec. 4. We conclude the paper in Sec. 5.

2. Differential signal coupler

A differential signal coupler is a device designed to decouple differential signal from a pair of coupled lines (Fig. 1a) [1]. The pair of microstrip lines (1-2 and 3-4) guides the differential signal V_d defined as a difference of signals in lines 1-2 and 3-4. The branches (5-6 and 7-8) decouple the part of signal from the main lines (branch 5-6 from line 4-3 and 7-8 from 1-2 respectively). The entire differential signal coupler can be considered as a combination of two independent classical proximity couplers located on both sides of the transmission line with offset along the main transmission line [11]. This configuration allows us to eliminate the undesired capacitances between branches. The total guided signal V_d can be represented as a set of two components defined as signals V_1 and V_3 between the common ground plane and the corresponding wires. Signals V_1 and V_3 have the same amplitudes and opposite phases. In the far field area, the sum of V_1 and V_3 is zero. Let us define the following coupling factors in [dB] for coupling phenomena between the neighboring paths: C_L, C_{52}, C_{54}, C_{73}, C_{71} (Fig. 1a).
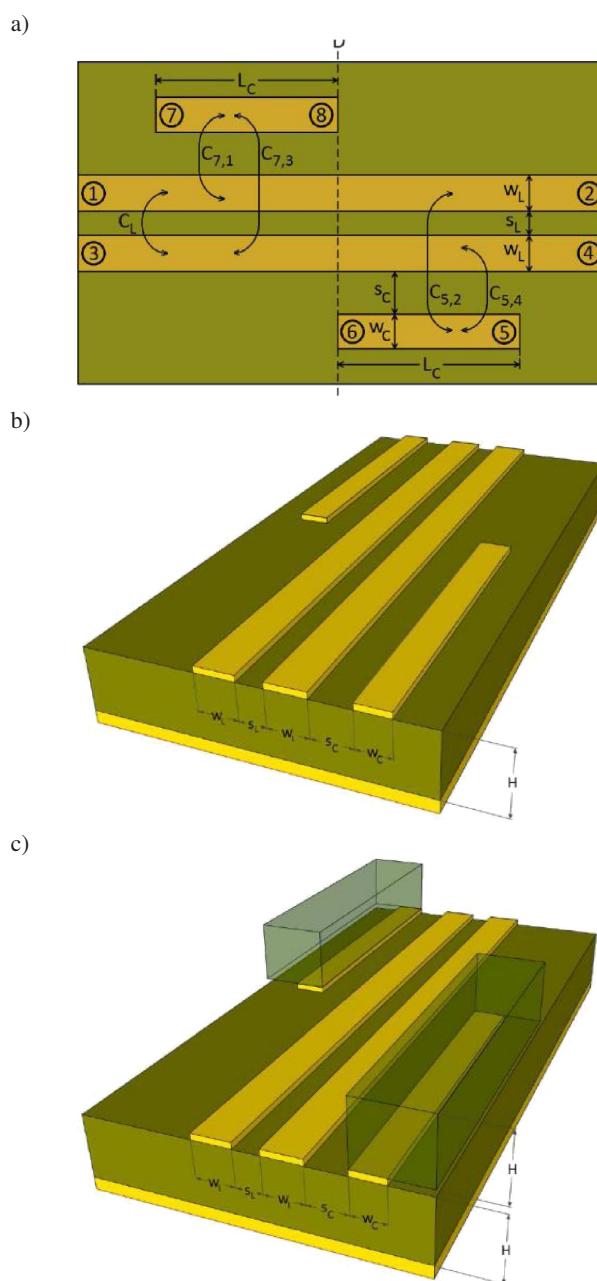
a)

b)

c)

Fig. 1. Differential signal coupler: (a) concept, (b) realization for microstrip technology, (c) equivalent structure to (b) where elements of coupler are fabricated on the separate parts of laminate and are overlayed on PCB under test after Ref. 2

Geometrical relations between the dimensions of the transmission line and the coupling strips allow us to assume that $C_{52} < C_{54}$, and, analogically, $C_{73} < C_{71}$. Let us define an additional signal V_d' as the difference between the signals at points 6 and 7, and assume that $V_d' \sim V_d$. Geometrical dimensions of the coupling lines, s_C, w_C and L_C, are determined by the desired differential coupling factor C_{diff} (defined as a coupling factor between a differential transmission line port 1-3 and a coupler output port 6-7) for a given frequency with minimal coupler impact on the transmission line. As demonstrated in [1, 11] (through theoretical considerations, simulations and frequency domain measurements), by taking into

account aforementioned assumptions it is possible to design a differential signal coupler which does not affect the transmission in the main line with the desired level of decoupling, using well known synthesis methods described in [13, 14]. Let us assume that the coupling factors for both branches are equal ($C_{54} = C_{71} = C_B$). Impedances for the even Z_e and odd Z_o modes for the pairs of single coupling branch and single strip of the transmission line (line 1-2 and branch 7-8, line 3-4 and branch 5-6) with the assumed characteristic impedance Z, can be expressed as follows [14]:

$$Z_{0e} = \sqrt{\frac{1 + 10^{(C_B/20)}}{1 - 10^{(C_B/20)}}}, \qquad Z_{0o} = \sqrt{\frac{1 - 10^{(C_B/20)}}{1 + 10^{(C_B/20)}}},$$

where C_B is a forward coupling factor between a single coupling branch and a single closer line in [dB]. The distance s_C between the transmission line and the branch of the coupler can be determined using the dependencies below [13]

$$(s_c/h) = \frac{2}{\pi}\cosh^{-1}$$

$$\cdot \left\{ \frac{\cosh\left[\frac{\pi}{2}\left(\frac{w_c}{h}\right)'_{so}\right] + \cosh\left[\frac{\pi}{2}\left(\frac{w_c}{h}\right)_{se}\right] - 2}{\cosh\left[\frac{\pi}{2}\left(\frac{w_c}{h}\right)'_{so}\right] - \cosh\left[\frac{\pi}{2}\left(\frac{w_c}{h}\right)_{se}\right]} \right\},$$

where h is a PCB substrate height, $(w_c/h)_{se}$ and $(w_c/h)_{so}$ are auxiliary parameters for even and odd modes.

The parameter $(w_c/h)'_{so}$ is expressed as a sum of $(w_c/h)_{so}$ and $(w_c/h)_{se}$ with constant factors. Parameters $(w_c/h)_{so}$, $(w_c/h)_{se}$ are calculated by changing auxiliary parameter R to $(Z_{oo}/2)$ for $(w_c/h)_{so}$ and $(Z_{oe}/2)$ for $(w_c/h)_{se}$ in the equation [13]:

$$(w_c/h)_{se,\,so}$$
$$= \frac{8\sqrt{\left[\exp\left(\frac{R}{42.4}\sqrt{(\varepsilon_r+1)}\right) - 1\right]\frac{7 + (4/\varepsilon_r)}{11} + \frac{1 + (1/\varepsilon_r)}{0.81}}}{\left[\exp\left(\frac{R}{42.4}\sqrt{(\varepsilon_r+1)} - 1\right)\right]},$$

where ε_r is a dielectric constant of the substrate.

$$\left(\frac{w}{h}\right)'_{so} = 0.78\left(\frac{w}{h}\right)_{so} + 0.1\left(\frac{w}{h}\right)_{se}.$$

Finally, the w_c/h ratio can be specified as [14]

$$w_c/h = \frac{1}{\pi}\cosh^{-1}(d) - \frac{1}{2}\left(\frac{s_C}{h}\right),$$

$$d = \frac{\cosh\left[\frac{\pi}{2}\left(\frac{w_C}{h}\right)_{se}\right](g+1) + g - 1}{2},$$

$$g = \cosh\left[\frac{\pi}{2}\left(\frac{s_C}{h}\right)\right].$$

The length L_C of the coupling branch, which ensures a desired value of the coupling factor at the operating frequency f, is equal to a quarter of a wavelength in the substrate, λ [14]

$$L_C = \frac{\lambda}{4} = \frac{c}{4f\sqrt{\varepsilon_{eff}}}.$$

The total effective dielectric permittivity ε_{eff} can be calculated on the basis of an effective permittivity for even ε_{effe} and odd ε_{effo} modes

$$\varepsilon_{eff} = \left[\frac{\sqrt{\varepsilon_{effe}} + \sqrt{\varepsilon_{effo}}}{2}\right]^2.$$

These parameters strongly depend on capacitances between the conducting stripes and the ground plane, and the conductive stripes mutually [14]. The way of calculating permittivities for both modes with full capacitance calculations is shown below

$$\varepsilon_{effe} = \frac{C_e}{C_{e1}},$$

$$\varepsilon_{effo} = \frac{C_o}{C_{o1}},$$

where C_e, C_o are total capacitances for each mode and C_{o1}, C_{e1} are similar capacitances but with air as a substrate. It was shown in [1, 11] that physical construction presented in Fig. 1c, where the coupling branches are fabricated on separate PCBs and overlayed on the board with the line under test, can be treated with high level of accuracy as equivalent to the configuration of Fig. 1b. For practical reasons, the measurements presented in the following sections are performed using the topology of Fig. 1b. Because of the aforementioned equivalence, the conclusions drawn from our results are valid for both versions (Fig. 1b and Fig. 1c).

3. Coupler design and directivity optimization

As it is shown in [1, 2], the differential signal coupler of Fig. 1 (which satisfies the assumptions outlined in Sec. 2) can be designed as a pair of classical microstrip proximity couplers. The design can be conducted using well-known methods presented in [14]. Let us consider the pair of coupled microstrip which guides a differential signal on PCB. The line's coupling factor is $C_L = -15$ dB. For FR-4 laminate with $\varepsilon_r = 4.4$ and $H = 1.55$ mm, the single line width is $w_L = 2.88$ mm and the distance between there lines is $s_L = 0.67$ mm. We assume that the coupler will be used to decouple signals from the main line for which the significant part of the power is concentrated in the band below 1 GHz. We define the desired coupling factor at the operating frequency $f = 1$ GHz for a single transmission line strip and a coupler branch as -20 dB. This value was taken as a compromise between the two conditions: $C_L > -15$ dB and the probed signal amplification of 20dB for further signal processing is feasible. The coupling factor for frequencies lower than 1GHz is lower than -20 dB. This property implies that for real digital signals the natural pre-equalization will take place (the high frequency signal components with relatively low level of power will be enhanced in comparison to the lower frequency components). Using the design equations for classical couplers presented in [13, 14] we can calculate, for the FR-4 laminate with $\varepsilon_r = 4.4$ and $H = 1.55$ mm, the coupler's branch width $w_C = 3.02$ mm and the distance between transmission line and coupler's branch $s_C = 1.59$ mm. The length

of the coupler branch is $L_C = 41.33$ mm. The measurement results of the coupling characteristics for the designed coupler (Fig. 5b) are presented in Fig. 2. We can observe that the desired coupling factor at $f = 1$ GHz was obtained. The coupling factor has lower values for frequencies below f (-35 dB at 100 MHz, -28 dB at 200 MHz, -24 dB at 400 MHz). The measured coupler's isolation (which is a sum of directivity and coupling factor) is -24 dB at the working frequency $f = 1$ GHz. This value is not sufficiently small in comparison to the level of the coupler's coupling factor (-20 dB). The directivity determines the properties of the signal decoupling promoted to the main line in a particular direction. To improve the coupler's directivity, geometry optimization has been performed. The methodology of coupler's directivity optimization was based on considerations presented in [15]. To optimize the coupler geometry, we used the idea of stepped impedance microstrip coupler [15]. The coupler's geometry parametrization is shown in Fig. 3b. Initial dimensions have been obtained from analytical synthesis. The design optimization goals are shown in Fig. 4. The optimization was performed using the Quasi-Newton algorithm built in Agilent ADS. The Quasi-Newton search method uses second-order derivatives of the error function as well as its gradient to find a descend isolation [16]. The second order derivatives are estimated by the Davidson-Fletcher-Powell update formula. After optimization, the coupler's isolation was increased from -28 dB to -40 dB at $f = 1$ GHz (for lower frequencies the isolation is better). The improvement of directivity did not result in deterioration of other important parameters (coupler's match, transmission's line match, coupling factor). Furthermore, the total length of the coupler branch was reduced from $L_C = 41.33$ mm to 29.7 mm. The geometrical dimensions of optimized coupler are as follows: $w_{1C} = 0.67$ mm, $w_{2C} = 6.24$ mm, $s_1 = 4.92$ mm, $s_2 = 0.67$ mm, $L_{1C} = 9.9$ mm, $L_{2C} = 9.9$ mm (the symbols are consistent with those shown in Fig. 3b).
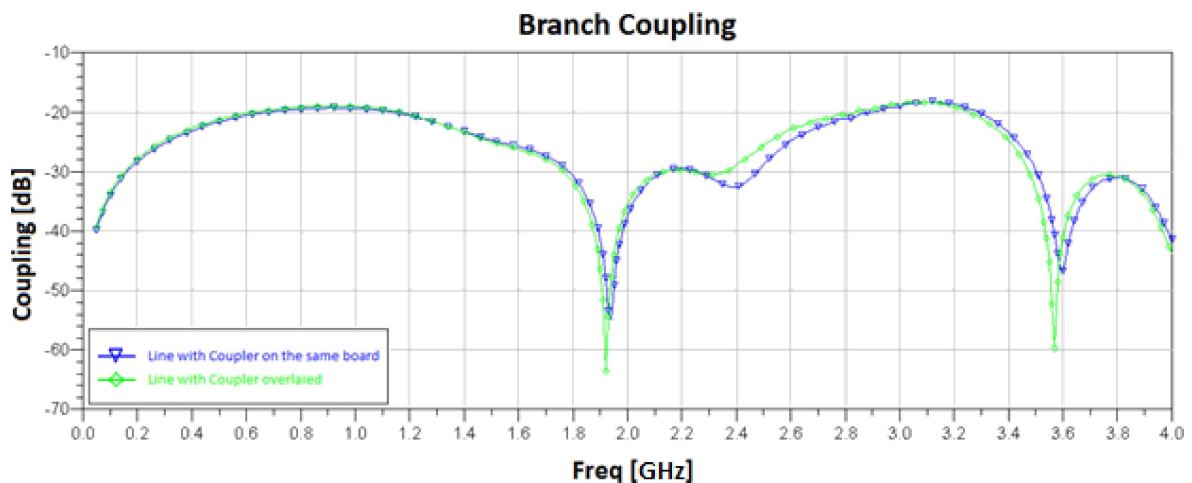

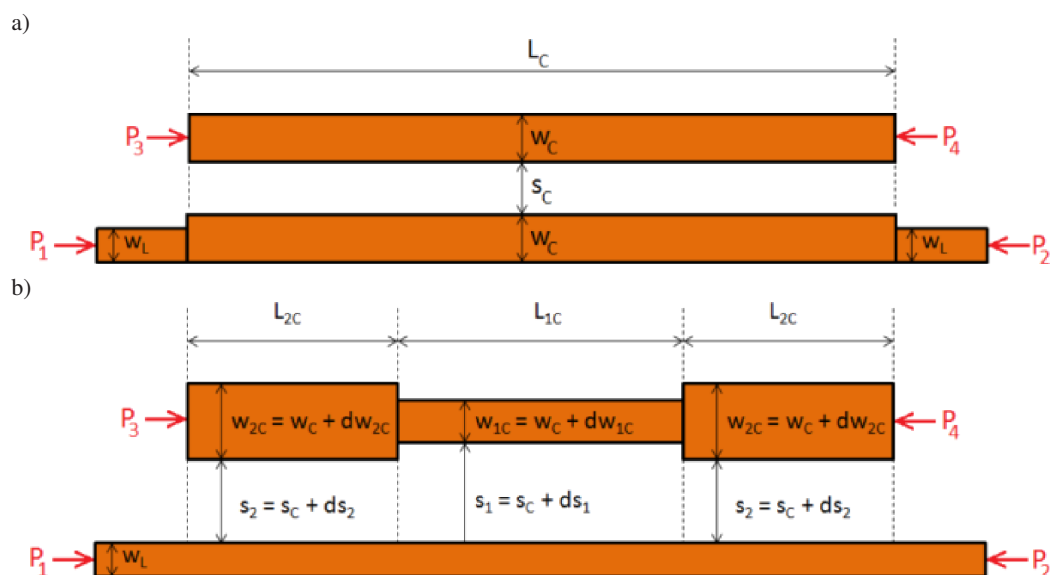Fig. 2. Coupler's branch coupling characteristic (Agilent Technologies E5071C VNA measurements)

Fig. 3. Single branch of microstrip directional coupler: (a) initial structure, (b) optimized stepped impedance geometry
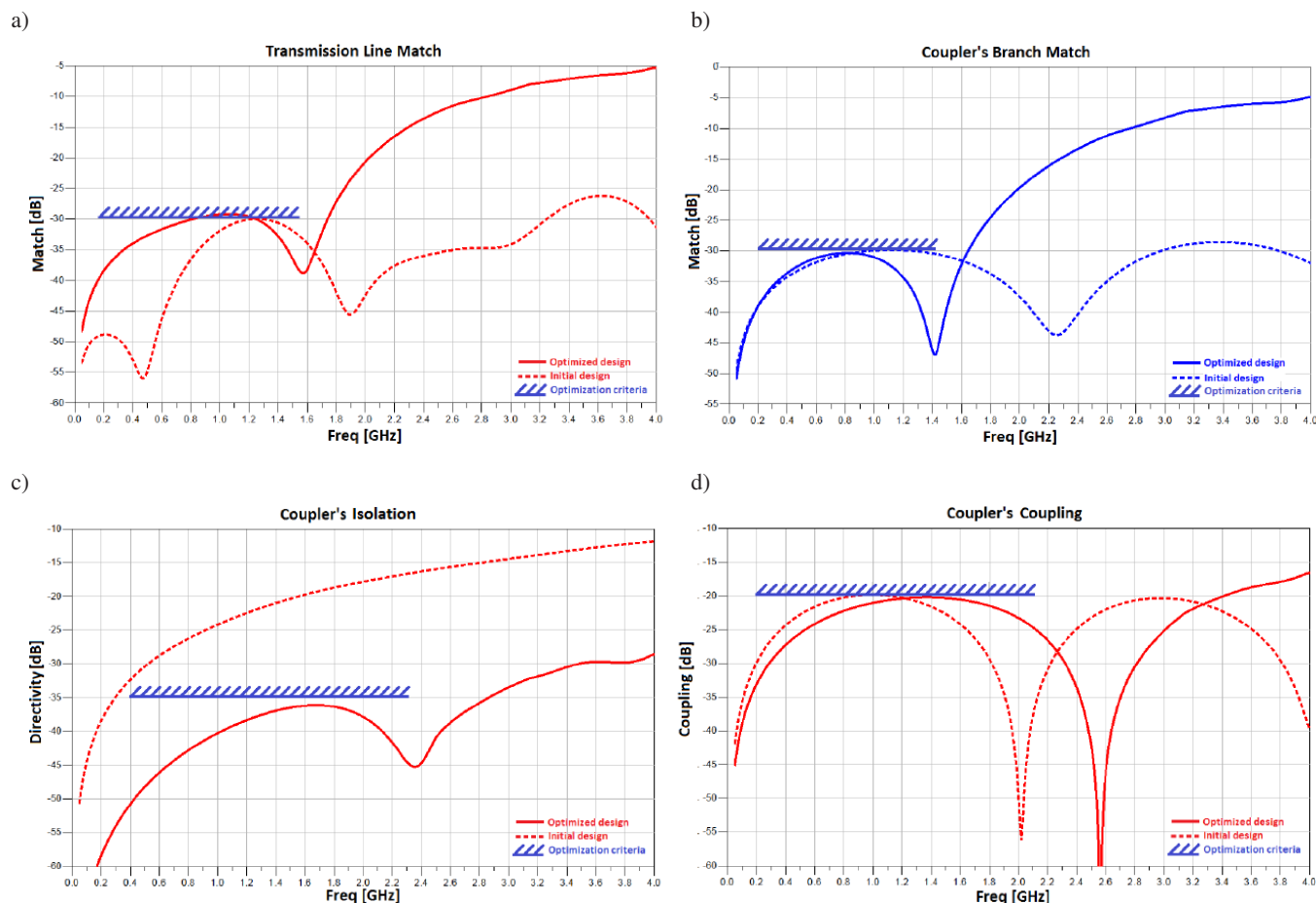
The contact-less method of chip-to-chip high speed data transmission monitoring

a)

b)

c)

d)

Fig. 4. Directional coupler optimization goals and the optimized responses compared to those of the initial design

4. Measurements

This section presents the time domain measurements of the differential signal couplers with real signals transmitted between digital integrated circuits on the motherboard (Fig. 5) The block diagram of the measurement test set is presented in Fig. 6. The signal is transmitted from the transmitter Tx to the receiver Rx through the transmission line. The transmitter generates differential signal with amplitudes 0.5 V in reference to the ground which results in amplitude 1 V between the coupled lines. The differential signal coupler is placed in the middle of the transmission line. All ports of the differential signal coupler are terminated with the matched 50 Ω load. The signals are observed in the measurement points as follows: V_i – input signal for the single micristrip line, V_T – the signal decoupled from the transmission line in direction Tx-Rx, V_R – coupler's isolated port, V – a single transmission line output at the Rx side. For practical purposes, the three test boards were fabricated: the reference differential transmission line (Fig. 5a) and the other two with the transmission lines with differential signal couplers (designed directly using classical methods, Fig. 5b and the optimized one in Fig. 5c). All circuits were implemented on the low cost laminate FR-4 ($\varepsilon_r = 4.4$, $H = 1.55$ mm). The physically realized measurement test set is presented in Fig. 7. The transmitter and the receiver were realized on the basis of the Xilinx ML605 de-

velopment kit [12]. The board contains Virtex-6 FPGA with 512MB RAM DDR3, 128Mb platform flash and four Multi-Gigabit SMA ports. The measured signals were observed with the Agilent InfiniiVision 7000B series oscilloscope. Additionally, the spectrum of Tx output signal was measured with the Agilent X-Series Signal Analyzer N9000A. The measurements were performed for the two representative transmission rates: 200 Mb/s and 333 Mb/s. The measurement results are presented in Fig. 8. As we can observe, the significant part of the input signal power for both cases is concentrated in the frequency band below 1 GHz. For 200 Mb/s transmission, the delay in the transmission line is 1.5 ns. The amplitude of the signal V_o at the Rx side is 0.05 V lower than on the V_i Tx side. Additionally, the shape of the signal is slightly distorted. The same results were obtained for all three test boards: the reference transmission line and the transmission line with couplers. This indicates that the designed differential signal couplers do not disturb transmission under test. For 333 Mb/s, the transmission delay has the same value as for 200 Mb/s (1.5 ns). For this case, the amplitude of the signal V_o on the Rx side is more significantly reduced (by about 0.2 V). The measured waveforms were identical for all three boards, which prove that the couplers do not disturb transmission in the main line for 333 Mb/s either. The signal from the coupled port V_T for 200 Mb/s transmission has visible

M. Zmuda, S. Szczepański, S. Kozieł, and S. Graczyk

peaks at the moments when there is a rising or falling edge in the main transmission line. The amplitude of V_T is 45 mV. This value is sufficiently high to be processed. The peaks are significantly more clear for the optimized version of the cou-

pler (the one with higher directivity). For both cases, it is possible to recover the information about the data transmitted in the main line on the basis of the signal decoupled by the differential signal coupler.

a)

b)

c)
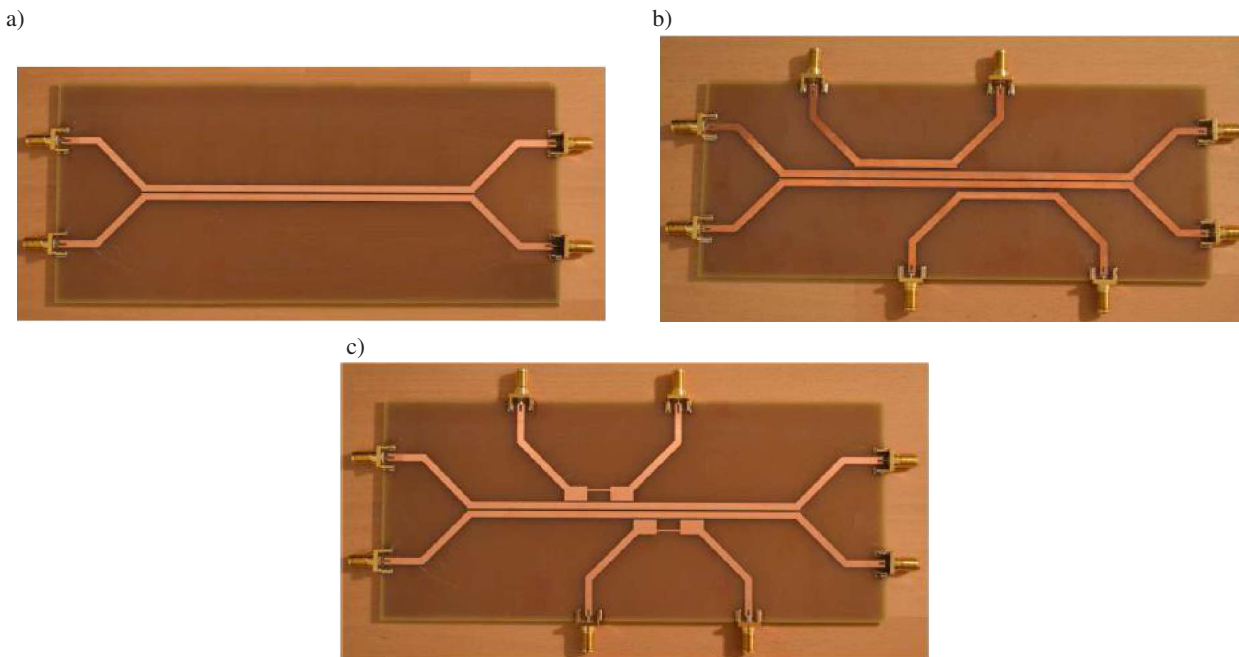
Fig. 5. Three test boards: (a) reference transmission line, (b) transmission line with differential signal coupler, (c) transmission line with optimized differential signal coupler (improved directivity)
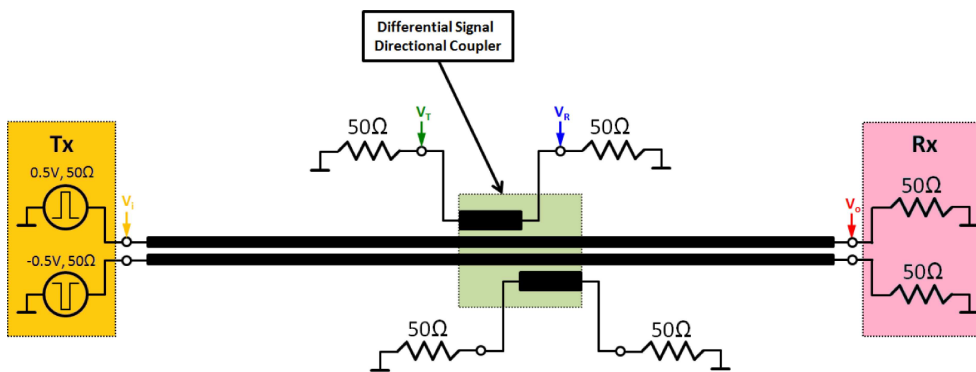
Fig. 6. Block diagram of measurement test set
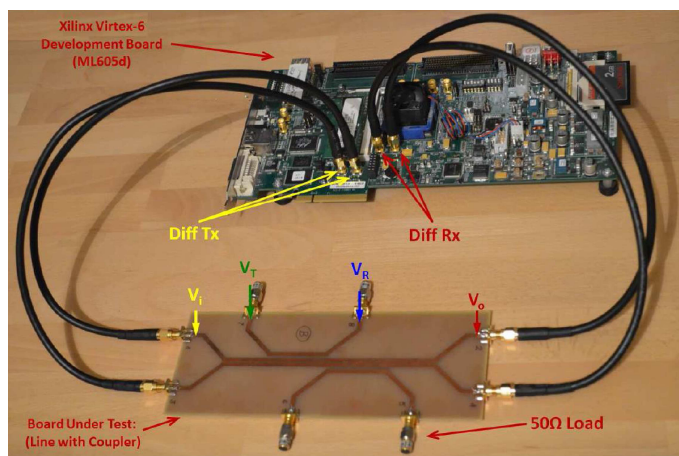
Fig. 7. Measurement test set: Xilinx Virtex-6 FPGA development board with transmission line under test and differential signal coupler
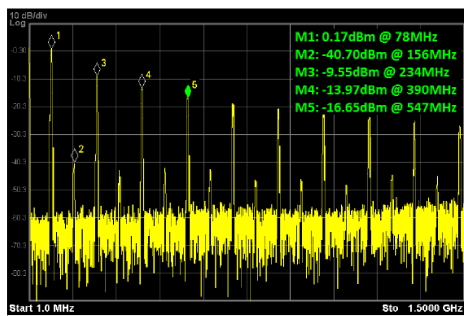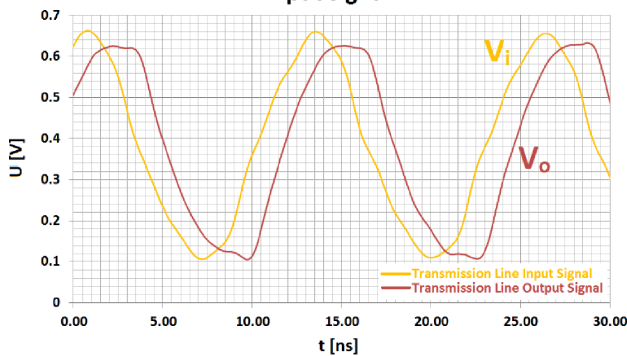
a)

b)

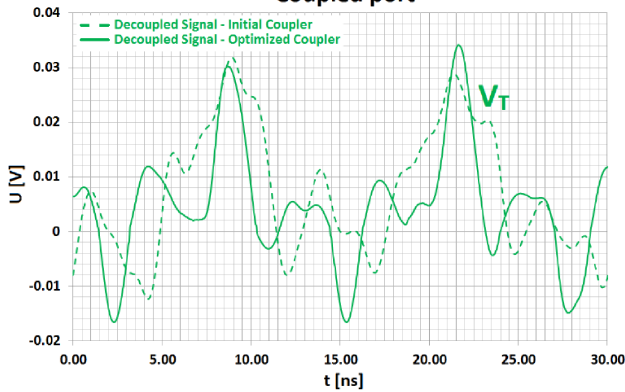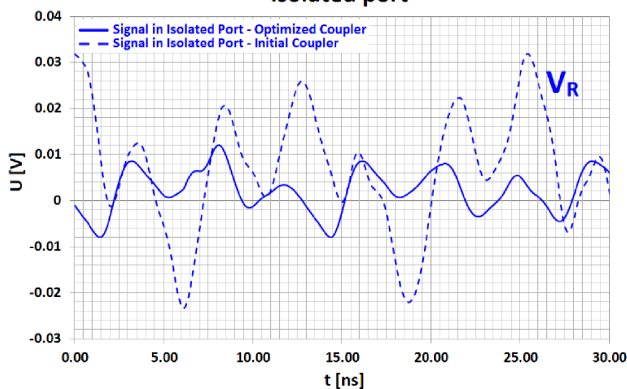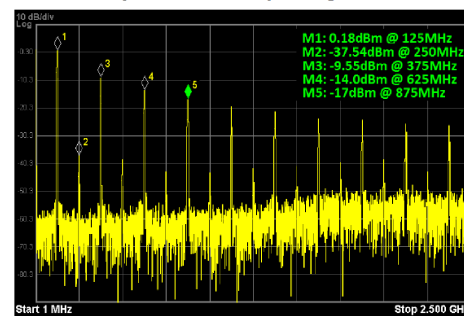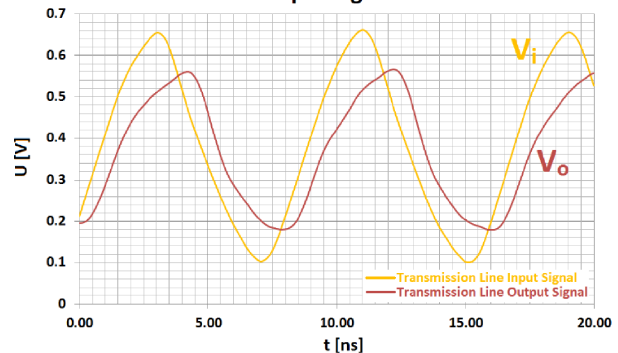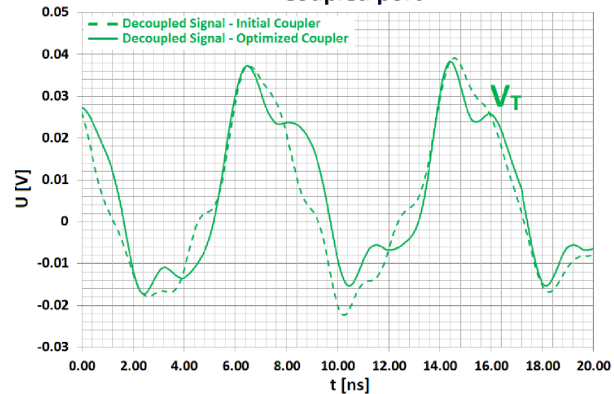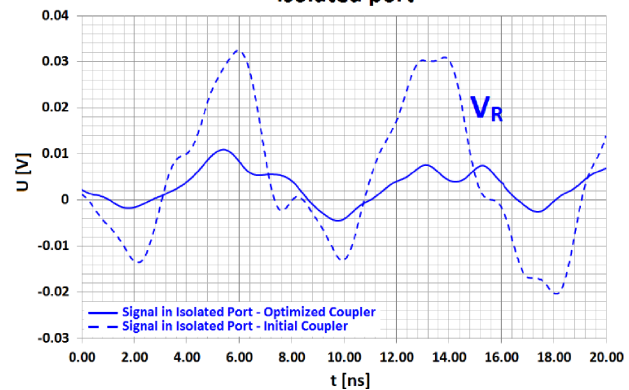Fig. 8.   Time domain measurements results for two transmission rates: a) 200 Mb/s and b) 333 Mb/s

The signal in the isolated port V_R should be equal to 0 for the ideal coupler. For initial version of the coupler, the amplitude of the signal in the isolated port is comparable with the amplitude of the signal in the coupled port. The situation is greatly improved for the coupler with optimized directivity. The decoupled signal waveform V_T for 333 Mb/s transmission looks completely different. The amplitude of $V_T = 60$ mV is higher than for 200 Mb/s transmission. The reason for this is that the major part of the signal spectrum 333 Mb/s is located at higher frequencies where the coupler's coupling coefficient is higher. Due to the short duration time of the Tx pulses V_i with smooth slopes, the coupled impulses caused by the rising and falling edges overlap. However, it does not preclude the possibility of recovering information about the signal transmitted in the main line on the basis of the signal decoupled by the differential signal coupler. For 333 Mb/s case, similarly as for the 200 Mb/s case, the signal in the isolated port V_R has much lower level for the configuration using the coupler optimized for directivity. As mentioned before, based on the research done by the authors in [1], due to equivalence of the structures presented in Fig. 1b and Fig. 1c, the aforementioned phenomenon observed for the structure from Fig. 1b will also occur in the structure of Fig. 1c. This conjecture confirms the possibility to monitor differential signal transmission in the coupled pair of microstrip lines on PCB using the coupler realized on the separate parts of the laminate and overlayed on PCB with the transmission lines under test.

5. Conclusions

In this paper, the technique of decoupling the differential signal transmitted in a pair of microstrip lines on PCBs with the dedicated coupler for high speed data transmission monitoring in chip-to-chip interconnections is presented. The method of coupler's directivity optimization which allows to improve the signal probing capabilities in comparison with its initial structure presented in [8] was proposed. The correctness of our theoretical considerations have been confirmed by the time-domain measurements carried out for real chip-to-chip communication signals using a dedicated measurement system. The results confirm that it is possible to monitor differential signal transmission in the coupled pair of the microstrip lines on PCB with the coupler realized on the separate parts of the laminate and overlayed on PCB with the transmission lines under test. Our results also indicate that improving the coupler's directivity through modified topology and optimized dimensions, significantly improves the conditions of recovering the signal transmitted in the main line. The presented technology can be used for reducing the cost of the product diagnostics by eliminating dedicated measurement connectors, run-time system debugging or reverse engineering.

REFERENCES

[1] W. Bandurski, *Analysis and Simulations of Highspeed Data Interconnections in High-speed Digital Circuits*, Poznań University of Technology Publishing House, Poznań, 2006, (in Polish).
[2] H.S. Sangha and C.A. Ridgeway, "Making the move to serial buses", *EDN Magazine* 3, CD-ROM (2005).
[3] M. Hosman, "High-speed bus debug and validation test challenges", *IEEE/SEMI Int. Electronics Manufacturing Technology Symp* 1, 218–222 (2004).
[4] Z. Zilic and Y. Fan, "A versatile scheme for the validation, testing and debugging of high speed serial interfaces", *IEEE Int. High Level Design Validation and Testing Workshop* 1, 114–121 (2009).
[5] P. Szymański and E. Sędek, "S-band MMIC 6-bit phase shifter", *17th Int. Conf on Microwave, Radar and Wireless Communications, MIKON* 1, CD-ROM (2008).
[6] A. Rysin, P. Livshits, S. Sofer, O. Mantel, Y. Shapira, and Y. Fefer, "Inter-Symbol Interference (ISI) in on-die transmission lines", *IEEE Int. Conf. on Microwaves, Communications, Antennas and Electronics Systems* 1, 1–5 (2009).
[7] G. Edlund, G. Lawday, and D. Ireland, *A Signal Integrity Engineer's Companion. Real-Time Test And Measurement and Design Simulation*, Prentice Hall Signal Integrity Library, London, 2008.
[8] E.A. Daoud and N. Nicolici, "Real-time lossless compression for silicon debug", *IEEE Trans on Computer-Aided Design of Integrated Circuits and Systems* 28, 1387–1400 (2009).
[9] TLA7Axx Logic Analyzer Modules, Tektronix (2010).
[10] M. Zmuda, S. Szczepański, and S. Kozieł, "A new coupler concept for contactless high-speed data transmission monitoring", *IEEE Trans on Instrumentation and Measurement* 62, 1–7 (2012).
[11] M. Zmuda, S. Szczepański, and S. Kozieł, "Design of novel microstrip directional coupler for differential signal decoupling", *IET Microwaves, Antennas & Propagation* 6, 721–728 (2012).
[12] ML605 Hardware User Guide, Xilinx Inc. (2012).
[13] A. Eroglu and J.K. Lee, "The complete design of microstrip directional couplers using the synthesis method", *IEEE Trans. on Instrumentation and Measurement* 57, 2756–2761 (2008).
[14] K.C. Gupta, R. Garg, and R. Chadha, *Computer-Aided Design of Microwave Circuits*, Artech House INC, London, 1981.
[15] J. Muller, C. Friesicke, and A. Jacob, "Stepped impedance microstrip couplers with improved directivity", *Int. Microwave Symposium Digest, MTT'09* 1, 621–624 (2009).
[16] *Tuning, Optimization and Statistical Design*, Agilent ADS User Guide, Palo Alto, 2009.